ARTICLE

doi:10.1038/nature11618

Hippocampal–cortical interaction during periods of subcortical silence

N. K. Logothetis[1,2], O. Eschenko[1], Y. Murayama[1], M. Augath[1], T. Steudel[1], H. C. Evrard[1], M. Besserve[1,3] & A. Oeltermann[1]

Hippocampal ripples, episodic high-frequency field-potential oscillations primarily occurring during sleep and calmness, have been described in mice, rats, rabbits, monkeys and humans, and so far they have been associated with retention of previously acquired awake experience. Although hippocampal ripples have been studied in detail using neurophysiological methods, the global effects of ripples on the entire brain remain elusive, primarily owing to a lack of methodologies permitting concurrent hippocampal recordings and whole-brain activity mapping. By combining electrophysiological recordings in hippocampus with ripple-triggered functional magnetic resonance imaging, here we show that most of the cerebral cortex is selectively activated during the ripples, whereas most diencephalic, midbrain and brainstem regions are strongly and consistently inhibited. Analysis of regional temporal response patterns indicates that thalamic activity suppression precedes the hippocampal population burst, which itself is temporally bounded by massive activations of association and primary cortical areas. These findings suggest that during off-line memory consolidation, synergistic thalamocortical activity may be orchestrating a privileged interaction state between hippocampus and cortex by silencing the output of subcortical centres involved in sensory processing or potentially mediating procedural learning. Such a mechanism would cause minimal interference, enabling consolidation of hippocampus-dependent memory.

Episodic memory—that is, memory of places, specific events and their contexts—depends on a synergistic interaction between anatomically related structures within the medial temporal lobe and the neocortex[1–3]. The process of consolidating such memories occurs in two consecutive steps that both involve an interplay between hippocampus and cortex[4–7]. During the encoding phase, hippocampus rapidly binds neocortical representations to local memory traces, while during subsequent 'off-line' periods of calmness or slow wave sleep (SWS) the new labile traces are concurrently reactivated in hippocampus and cortex to potentiate the corticocortical connections underlying stored representations[5,8].

An increasing number of studies support the view that the memory reactivation phase may be partly instantiated in the occurrences of so-called sharp wave-ripple (SPW-R) complexes[9,10], which are prominent during the off-line states. SPW-Rs are aperiodic, recurrent instances of large deflections (sharp waves) in the hippocampal local-field potential, and they are associated with synchronous fast-field oscillations (ripples), whose frequency depends on anatomical site (for example, CA1, CA3 or entorhinal cortex), animal state (alert or anaesthetized) and animal species[9–13]. Many of the ripple properties support the idea that SPW-Rs may indeed be involved in off-line memory consolidation[5,14]. Their intrinsic frequency and temporal structure are optimal for inducing synaptic plasticity in downstream neurons. Moreover, SPW-Rs have a global nature, reflecting the activation of hippocampal subnetworks and a behaviourally relevant spike content. For example, reactivation of neuronal ensembles that were active during awake experience occurs primarily during ripples[15–18], the number of ripples increases after learning, and the increase seems to predict memory recall both in rats[19–21] and in humans[12]. Conversely, elimination of ripples by the electrical stimulation of hippocampus during the post-learning SWS interferes with memory consolidation[22,23].

It is worth noting that SPW-Rs are not idiosyncratic hippocampal episodes, but part of a large-scale complex system of many oscillatory networks, the coupling of which coordinates specific information transfer between neocortical and hippocampal cell assemblies[24–27]. One prominent self-organized oscillatory network involves thalamic and cortical structures, and generates the pattern of slow oscillation[28,29]. During this slow (0.5–1.5 Hz) oscillation, the membrane potential of both excitatory and inhibitory cells alternates between depolarized (up) and hyperpolarized (down) states, and these excitability phases and their transitions strongly affect the frequency of occurrence of other cortical[30,31] and hippocampal[27,32,33] oscillatory patterns. Specifically, SPW-Rs are temporally linked to cortical spindles[24,34,35], and therefore their frequency of occurrence also correlates with slow oscillations[27,33]. It has been suggested that the slow-oscillation network mentioned above underlies off-line information processing and that it has properties that are affected by learning[36,37].

Clearly, such organization suggests that memory consolidation is a complex system property emerging from the concerted, context-dependent operations of micro- and macro-networks of the brain. In such systems, the organization and operational principles of complex systems may be better investigated by using multimodal approaches, including concurrent measurements on multiple spatio-temporal scales. Here we used a novel multimodal methodology, which we call neural-event-triggered functional magnetic resonance imaging (NET-fMRI), to record ripples physiologically in the rhesus monkey (*Macaca mulatta*) and use them as events to align and average the time courses of brain activations (see Supplementary Methods). Concurrent multi-site hippocampal recordings and whole-brain fMRI were conducted during epochs of spontaneous activity or electrical stimulation of the CA1 and CA3 hippocampal fields to investigate the full extent of brain regions whose activity is modulated at times of ripple occurrence.

[1]Max Planck Institute for Biological Cybernetics, Spemannstraße 38, 72076 Tuebingen, Germany. [2]Centre for Imaging Sciences, Biomedical Imaging Institute, The University of Manchester, Manchester M13 9PT, UK. [3]Max Planck Institute for Intelligent Systems, Spemannstraße 38, 72076 Tuebingen, Germany.

Identification of SPW–R complexes in monkeys

Recording electrodes were positioned on the basis of individual, high-resolution structural MRI scans and online observation of neural response profiles (Supplementary Methods and Supplementary Fig. 1). Further classification of electrode contacts in pyramidal-layer and stratum radiatum was based on visual detection of oscillations and inspection of synchronous activity (Supplementary Fig. 2).

Figure 1a shows two typical examples of SPW-R complexes. The upper traces depict the denoised broadband (0.05–500 Hz) field-potential signals, each showing at least one characteristic sharp wave. Consistent with previous studies[9,11,38], the duration of the ripple events was found to be less than 100 ms, and the sharp wave deflections had an amplitude of 1–3 mV. The lower traces show the bandpass (80–180 Hz)-filtered derivative of the signal with the fast ripple oscillations associated with sharp waves. The amplitude of ripples was approximately one order of magnitude smaller than that of concurrent sharp waves. SPW-Rs were always synchronous in most recorded sites, with maximum SPW amplitude mainly within the stratum radiatum and clear oscillations within the pyramidal cell layers (Supplementary Fig. 2).

In a large number of previous studies, ripples were commonly detected by first bandpass filtering (for example, 100–250 Hz) the field potential, then rectifying, smoothing and normalizing the derivative signal, and finally detecting suprathreshold signal increases. But this methodology does not discern ripple-related increases in the high-frequency domain from those that may occur in a broader frequency band. In fact, it was recently shown that fast field-potential oscillations of rat hippocampus during sleep or immobility may be split into quantitatively distinct oscillatory patterns, high-gamma-frequency oscillations and ripple oscillations, reflecting the activity of distinct subnetworks[38]. To better understand the relationship of ripples to whole-brain activity, candidate oscillatory events were first detected by examining the smoothed envelope of the broadband (10–180 Hz) local-field potential (LFP) (see Supplementary Methods). To identify potentially distinct neural events, we next computed the wavelet spectra of peri-event segments of this signal in a window of −200 to 200 ms and separated them into clusters using an un-supervised feature-extraction algorithm (see Supplementary Methods), permitting decomposition of multivariate data into a user-defined cluster number. Applying the algorithm to all data for different cluster numbers (between two and five) disclosed that the best factorization is obtained with a cluster number of three, yielding three distinct event categories in the frequency domains of 8–22 Hz, 25–75 Hz and 80–180 Hz, referred to here as hpsigma (the range of hippocampal sigma waves), gamma and ripple bands, respectively. The average time–frequency representation of these clusters are shown in Fig. 1b for all sessions with anaesthetized animals. The average peak frequencies of the hpsigma, gamma and ripple spectra were 13.5 ± 1 Hz (mean ± s.d.), 40.1 ± 13 Hz and 106.5 ± 23 Hz, respectively. The average event durations (full width at half maximum, FWHM) were 226 ± 12 ms, 93 ± 22 ms and 44 ± 4 ms. The corresponding frequency peaks in drug-free experiments (Supplementary Fig. 3a) were 16 ± 3 Hz (mean ± s.d.), 40.5 ± 18 Hz and 106.8 ± 17.8 Hz, and the event durations were 199 ± 28 ms, 89 ± 26 ms and 40 ± 15.3 ms. Frequency ranges and time durations were determined by calculating the time–frequency decomposition of the suprathreshold (>1 s.d. of event-free intervals) signals and subsequently computing the FWHM. Consistent with previous studies, the oscillation frequency of monkeys and human ripples was lower than in rats, and the event duration was shorter[9–13].

To assess further the distinctiveness of the three event types, we examined their relationship to hippocampal slower oscillations such as the delta band. The relationship of each of the three identified events to the delta phase are shown in Fig. 1c (see also Supplementary Methods), with data displayed in the form of polar plots and histograms to assist visualization. A statistically highly significant phase locking was specific to the ripple events (Rayleigh test; $Z = 7.5$, $P < 0.004$). The orange histograms in the background show the phase distribution of random events (defined by the permutation of inter-event intervals) with their respective Rayleigh values of $Z = 0.5$ and $P < 0.519$, indicating a random distribution of

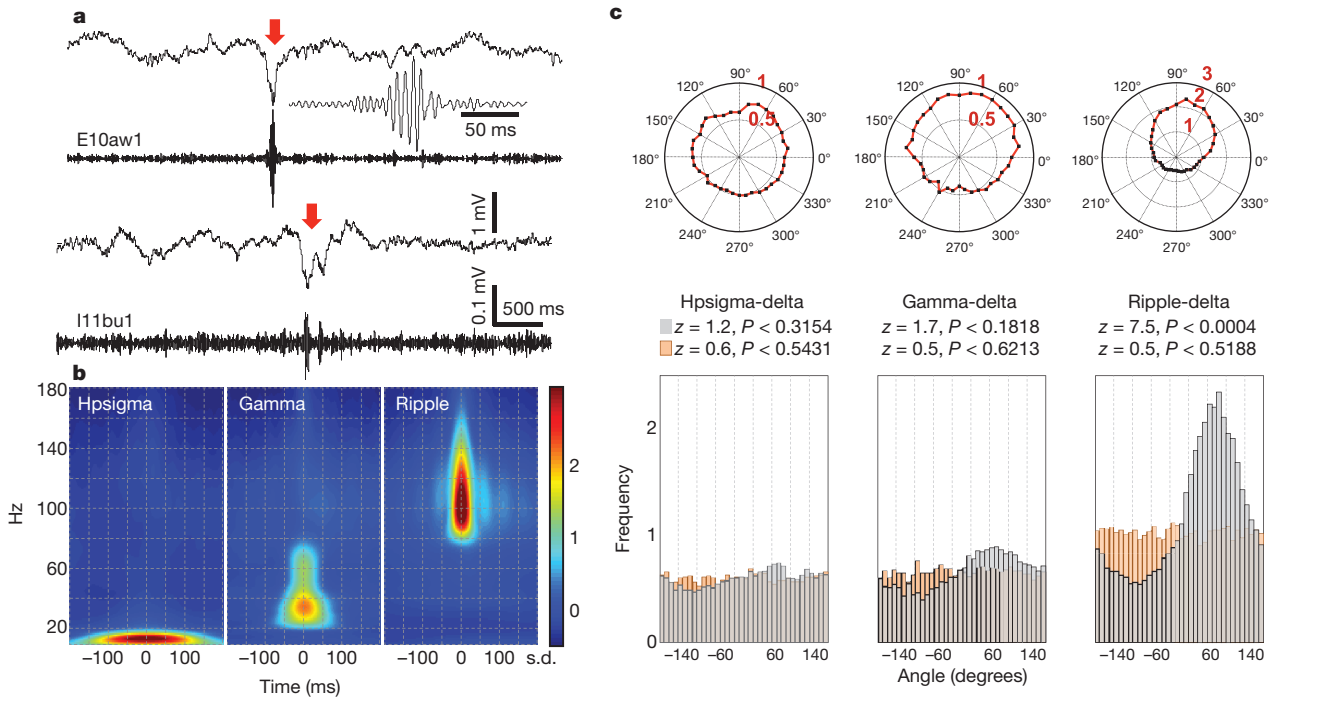

Figure 1 | Sharp wave–ripple complexes. **a**, SPW-Rs from two monkeys (i11, E10). Broadband (0.05–500 Hz) LFP signal (top panel) with (MRI) noise removed, together with their bandpassed (80–180 Hz) derivatives (bottom panel). Arrows show SPW-R. The ripple in the E10aw1 trace is magnified in the inset. **b**, Overall average of complex Morlet-wavelet spectrograms, showing the time–frequency distribution of hpsigma, gamma and ripple events. **c**, Cross-frequency coupling of hippocampal events and hippocampal delta-band activity. Results are shown as polar plots (top row; red, frequency of occurrence) and standard histograms (bottom row). Dark histograms are from event-triggered data. The orange histograms in the background reflect phase distribution from random events.

phases. The mean delta-phase value at which ripples occurred was close to 90° (84°), that is, preceding but close to the positive–negative transition of the hippocampal delta wave (see also the average peri-ripple field potential changes in Supplementary Fig. 4a). Similar results were obtained in the awake monkey experiments (Supplementary Figs 3b and 5a).

We then examined the ripple-associated whole-brain activation patterns using NET-fMRI. Based on the detection and classification criteria described above, we observed overall more than 5,000 hpsigma and gamma events, and more than 11,000 ripple events. However, given the slow nature of the blood-oxygen-level-dependent (BOLD) fMRI signal, we excluded short (<1 s) inter-event intervals and instead used 3,966 hpsigma, 4,191 gamma and 9,482 ripple events from all the anaesthetized animal sessions to align and average the fMRI time series. The average LFP time course for the events used for NET-fMRI are shown in Supplementary Figs 4 and 5, together with the distribution of their inter-event intervals for anaesthetized and awake animal experiments. In addition, Supplementary Fig. 6 shows the distinct nature of individual events by showing selective increases in one frequency range but not in the others.

Neural-event-triggered BOLD MRI

The aforementioned events were used to map brain response patterns associated with signal increases in each frequency band. Neural and fMRI time courses were aligned to the time of each event, and their averages were convolved with a haemodynamic response function (HRF) and subsequently used as regressors in a standard event-related design (see Supplementary Methods and Supplementary Fig. 6c, d). Statistical parametric mapping was then carried out to identify regions whose activity was modulated by the occurrence of the episodic events. To simplify the localization of different brain regions we grouped the detailed structure names of the monkey brain (Supplementary Fig. 10a–c) into group regions of interest (ROIs), taking into account both the functional specificity of structures and the spatiotemporal MRI resolution. For example, the visual area 4 (V4) complex includes the cortical regions V4, V4A, V4D, V4V, the juxtastriate area, the prostriate area and V4T of a standard monkey atlas[39].

Results from one fMRI session, under our standard remifentanil anaesthesia, show that there are widespread, strong increases in the BOLD signal within the hippocampal formation, occipital, sensorimotor, temporal and parietal cortical areas, and in prefrontal cortex (Fig. 2a, b). In contrast, subcortical structures, including basal ganglia, cerebellum, tectum, lateral geniculate nucleus (LGN) and other thalamic nuclei, showed highly significant and robust signal decreases (Fig. 2b). The patterns of activation and deactivation were highly consistent from subject to subject, and from session to session. Similar results were obtained with an un-anaesthetized animal (Figs 2c, d). Typically, the state of the monkey alternated between drowsy or asleep, and awake, with only infrequent mobility periods (for example, moving hands or licking the juice tube). The average ripple-triggered BOLD time courses for all sessions are displayed in Supplementary Figs 7b and 8b for the anaesthetized and awake animal, respectively.

Overall, ripples were related to both positive and negative BOLD responses (PBRs, NBRs). Unexpectedly, closer examination of these ripple-associated BOLD responses revealed that structures exhibiting PBR and NBR were grouped according to a specific anatomical

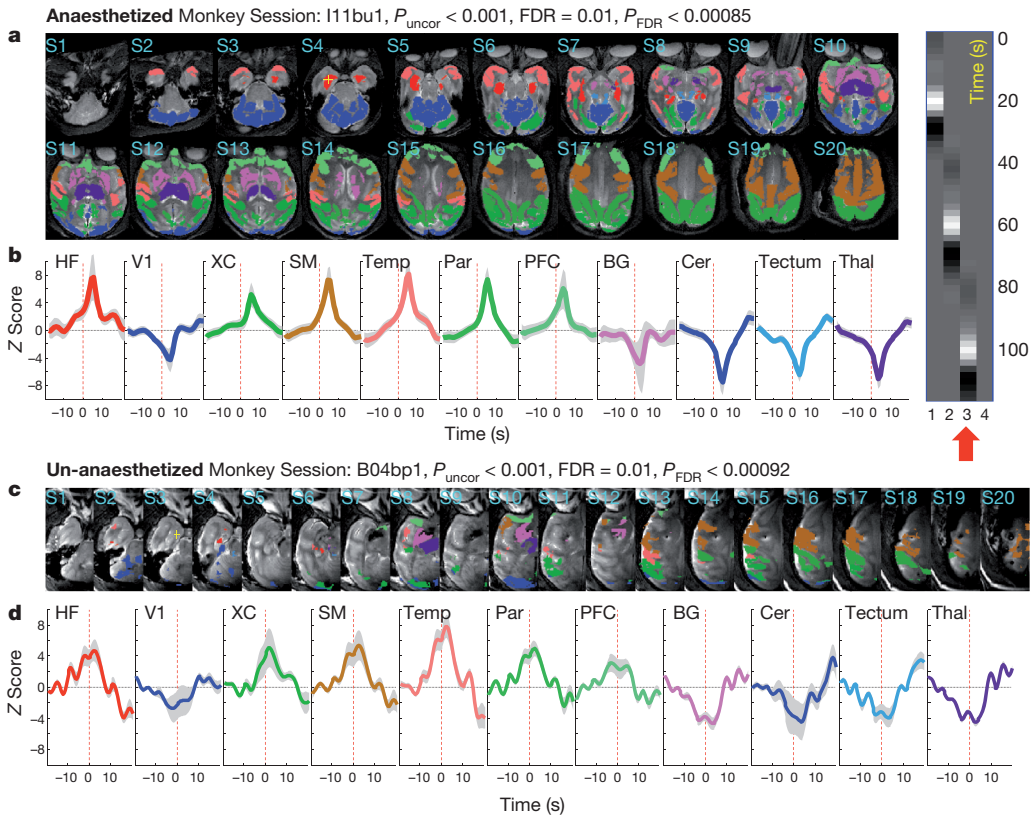

Figure 2 | Examples of ripple-triggered BOLD maps in anaesthetized and awake monkeys. **a**, BOLD maps obtained using NET-fMRI. Colours encode the selected group ROIs. Widespread activations were found in hippocampal formation (HF), extrastriate occipital areas (XC), sensorimotor cortex (SM), temporal (Temp) and parietal (Par) cortical areas, as well as in the prefrontal cortex (PFC). In contrast, subcortical structures, including basal ganglia (BG), cerebellum (Cer), tectum and thalamus (Thal), as well as the primary visual cortex (V1), showed robust signal decreases (see Supplementary Fig. 10 for ROI names). **b**, Average response in each of the aforementioned ROIs. Thick lines denote the mean of the BOLD time series and shaded areas show ±1 s.d. The inset (far right panel) shows the design matrix used in all experiments. The red arrow indicates the results obtained using the third regressor. **c**, **d**, Maps and time courses as in **a** and **b**, but for the un-anaesthetized animal (descriptions and conventions as in **a** and **b**). S, slice number. See Supplementary Methods for uncorrected (P_{uncor}) and corrected (P_{FDR}) statistical significance.

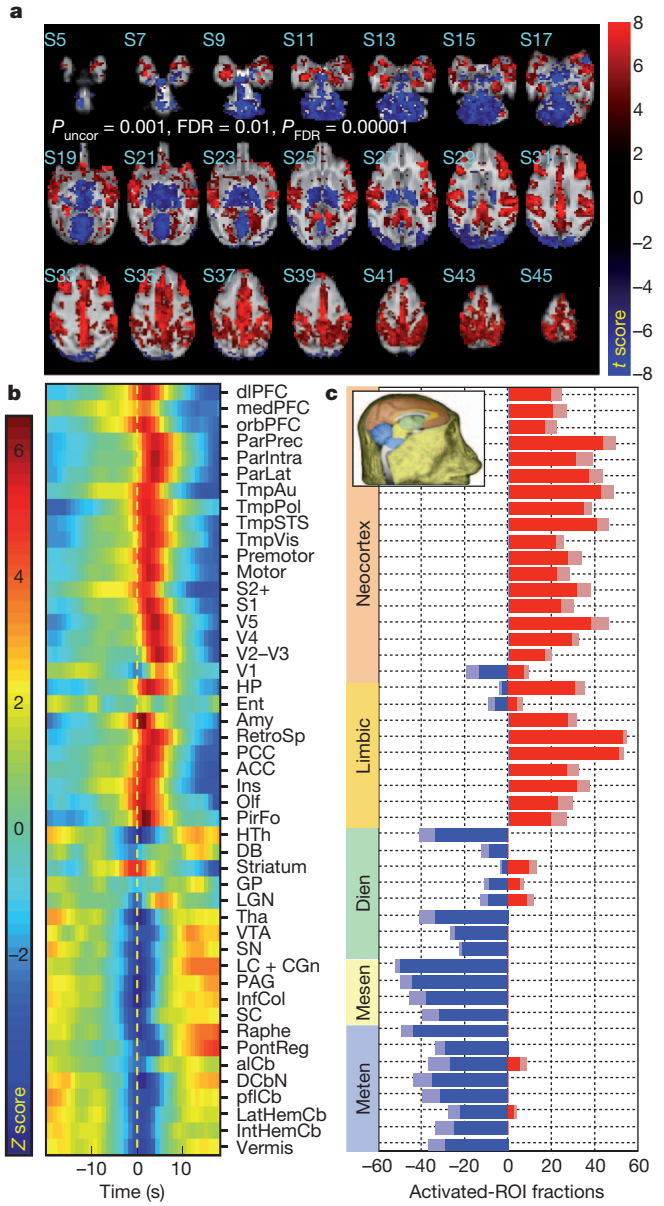

Figure 3 | Average ripple-triggered maps, signal dynamics and activation fractions. **a**, Average activation maps from all sessions. PBRs are observed in neocortex and limbic cortex, whereas activity suppression is seen in the diencephalon, mesencephalon and metencephalon. **b**, Time courses of each group ROI. In the stacked-bar plot, the lighter colour indicates +1 standard deviation. Note the sign change in the transition from cortical to subcortical areas and the difference in response onset. Dien, diencephalon; mesen, mesencephalon; meten, metencephalon. **c**, Fractions of activated voxels for each group ROI. ROIs are listed according to their location within the subdivisions of the standard developmental anatomical brain characterization, namely from the metencephalon (bottom) to the neocortex (top) (see Supplementary Fig. 10 for ROI names).

organization (Fig. 3a displays population data from all sessions, Supplementary Fig. 9 shows the averages of activation maps for each subject (see processing of population data in Supplementary Methods)). Similar to the maps of individual sessions, the population data showed that ripple-related PBRs occurred mainly in neocortex and limbic cortex, whereas activity suppression was observed in the diencephalon, mesencephalon and metencephalon. An almost unique exception to this selective activation–deactivation pattern was the primary visual cortex, V1, the activity of which was either unaffected by ripples or was suppressed (Supplementary Fig. 8e). The time courses of each group ROI (Fig. 3b) and the fractions of activated voxels for each group ROI (Fig. 3c) indicate that there is a dichotomy of response sign separating neocortex and limbic cortex from the other anatomical subdivisions.

Notably, this characteristic pattern of excitation–inhibition was entirely specific to ripple events. Gamma-associated modulations of brain areas were primarily increases in the BOLD signal (Fig. 4a, b) and of somewhat lesser extent, as can be seen in both the activation maps (Fig. 4a) and the activation fractions (Fig. 4c). Similarly, hpsigma-triggered fMRI gave primarily PBRs, albeit to a significantly lesser extent than those obtained with ripples (average gamma and hpsigma-triggered BOLD time courses for all sessions are displayed in Supplementary Figs 7c, d and 8c, d for anaesthetized and awake animals, respectively).

Timing analysis of ripple-triggered averages

The ripple-triggered average (RTA) responses, such as those shown in Fig. 3b, seemed to have an area-related onset time. We quantified this

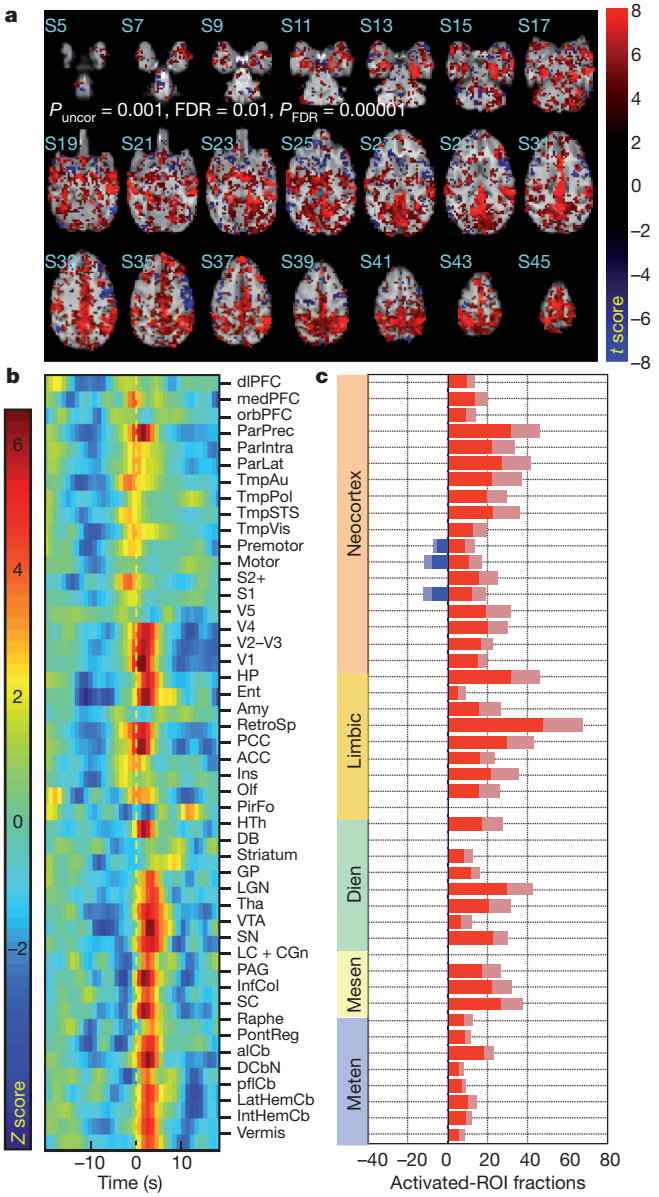

Figure 4 | Gamma-triggered population BOLD responses. Population results from NET-fMRI using gamma events to align physiological and fMRI responses. **a**, Average maps showing activations associated with gamma events. **b**, Time courses of the gamma-triggered BOLD response. Locations and names of ROIs are shown in Supplementary Fig. 10. **c**, Fractions of activated voxels for each group ROI. Conventions as in Fig. 3.

observation by calculating RTA responses for each ROI, clustering the responses and labelling the cluster according to the timing of their maximum (Sepplementary Methods). This analysis revealed a robust clustering of responses across sessions: an early RTA response (cluster 1) was characteristic of the frontal and prefrontal cortices, whereas a late RTA response (cluster 2) was mainly observed in sensory areas (Fig. 5a, b). The comparison of cortical RTA responses with hippocampal and thalamic responses revealed a sequential organization of activation and deactivation patterns for these group ROIs. Figure 5c shows the distribution of time points of maximum signal modulations across sessions. According to a pairwise *t*-test, thalamic deactivation seems to be the leading process and is followed by signal increases in temporal, prefrontal and other association cortices, then in hippocampus, and finally in parietal and early sensory cortices.

NET-fMRI seems to be an excellent tool for the study of dynamic and potentially effective connectivity. Other methods that could—in principle—be used to examine network topologies are direct electrical stimulation of the brain combined with fMRI or the non-invasive seed-based resting-state fMRI. To compare the outcomes of such methods with the NET-fMRI results presented here, we also conducted fMRI experiments during direct electrical stimulation (DES) of the CA1 or CA3 hippocampal field and studied the correlation maps obtained by resting-state fMRI using hippocampal seeds.

Connectivity with DES and resting-state fMRI

In the present DES studies, we chose stimulation parameters, such as current strength, burst amplitude and frequency, as well as the frequency of burst occurrence, similar to those calculated from ripple events (Supplementary Information and Supplementary Fig. 11). Typical activation maps obtained by electrical stimulation of the CA1 field are shown in Supplementary Fig. 12. Both activations and deactivations were observed in a number of different cortical and subcortical regions. However, the distribution of PBRs and NBRs was unrelated to that observed in the case of ripples, probably reflecting either the sustained negative BOLD[40] or synaptic distance and microcircuit organization[41] in the target structures (Supplementary Methods). Stimulation of the primate entorhinal cortex (Supplementary Fig. 12) with higher currents and stimulation frequencies entirely failed to induce trans-synaptic activations beyond hippocampus and entorhinal cortex itself.

Finally, the ongoing functional relationship of hippocampus to other cortical and subcortical brain regions was examined using standard seed-based resting-state fMRI. The left panel of Fig. 6 shows the average maps and the right panel shows the average fraction of activated ROI voxels for all sessions ($n = 7$) with hippocampus CA-field seeds. All significantly modulated ROIs, again barring V1 but also orbitofrontal cortex, exhibited strong positive BOLD responses that had a consistent spatial coverage across all sessions. Activated areas were the hippocampal formation, entorhinal cortex, the temporal, posterior cingulate and retrosplenial, prefrontal, olfactory and piriform cortices, as well as regions in thalamus and cerebellum. The cortical activations were similar to those reported in human studies[42], and were once again unaffected by anaesthesia.

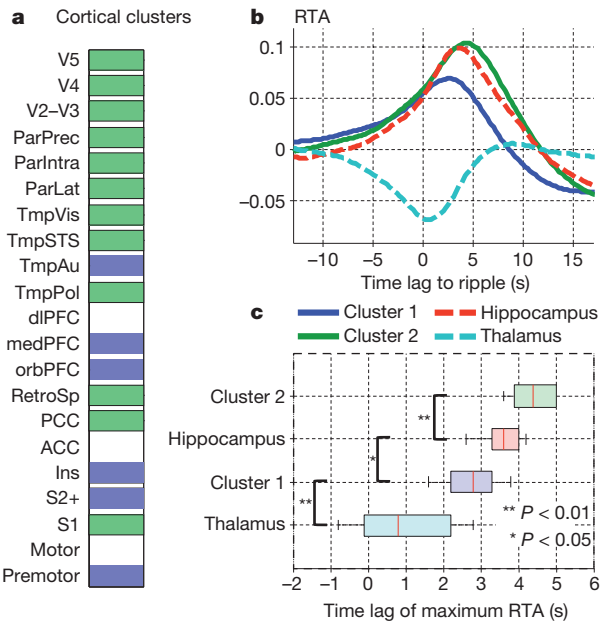

Figure 5 | BOLD response dynamics. **a**, Separation of the ripple-triggered average (RTA) responses in neocortical ROIs in two clusters. ROIs that do not belong significantly to either cluster are in white. **b**, Average RTA across all nine sessions for each cluster, superimposed on average hippocampal and thalamus responses. **c**, Box plot of the time lag until the maximum RTA is reached, for each cluster. On each box, the central mark is the median, the edges of the box are the 25th and 75th percentiles, and the whiskers indicate the most extreme data points. Asterisks, significant differences (*P*-values are given in the figure) between lags according to a one sided paired *t*-test (see Supplementary Fig. 10 for ROI names).

Discussion

Using NET-fMRI in anaesthetized and alert monkeys, we characterized here the brain areas that consistently increased or decreased their activity in relation to electrophysiologically detected and identified SPW-Rs. We show for the first time that the short periods of aperiodic, recurrent fast hippocampal oscillations (ripples) are tightly associated with robust cortical activations that occur concurrently with extensive activity suppression in subcortical thalamic, associational (for example, basal ganglia and cerebellum) and midbrain–brainstem neuromodulatory structures. The observed deactivations and activations were separated well spatially, so that previously described vascular steal phenomena or lateral and feedback interactions[40] can be safely excluded (see also Supplementary Information). This finding is specific to the ripple events and is not encountered in fMRI triggered by transient increases in the power of other frequency bands such as gamma and hpsigma. Moreover, the cortical–subcortical dichotomy of BOLD responses is observed neither during direct electrical stimulation of hippocampal fields, nor in resting-state fMRI using hippocampal seeds.

Markedly, during ripple episodes there seems to be a suppression of thalamic activity that might be related to sensory processing; a strategy

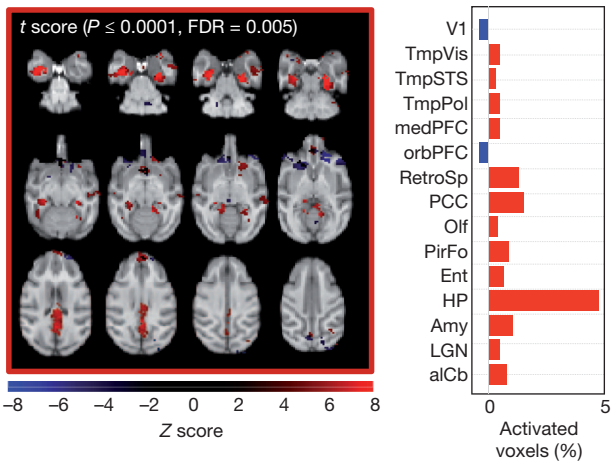

Figure 6 | Resting-state fMRI. BOLD maps (left panel) and the fraction of modulated ROIs (right panel). Resting-state fMRI with the hippocampus proper as the seed. Hippocampal formation, entorhinal cortex, temporal, parietal, prefrontal, olfactory and piriform cortices, as well as regions in thalamus and cerebellum are correlated with the ongoing hippocampus activity (see Supplementary Fig. 10 for ROI names).

that could increase the signal-to-noise ratio of hippocampal–cortical communication. In addition, there is a strong inhibition of large portions of the associational subcortical brain structures that are closely involved in the mechanisms of neural plasticity. For example, the deactivation of the basal ganglia, the pontine region and the cerebellar cortex seems to be consistent with prior evidence of competition between the fundamentally distinct declarative and non-declarative memory systems (see ref. 43 and discussion in Supplementary Information).

The majority of previous studies report competition between memory systems during the execution of various learning tasks, but evidence of post-learning antagonistic interactions between memory systems has also been reported in animal lesion and intra-hippocampal inactivation studies[44,45]. These findings suggested that competitive interference between multiple memory systems may in part occur during the memory consolidation period[46]. Such 'competition' may reflect an adaptive mechanism for optimizing behaviour that is dependent on learning demands, and its physiological basis is of paramount importance for both basic research and clinical applications. Evidently, the actual neuroanatomical interaction nodes between various memory systems that may underlie the deactivations observed here remain to be elucidated in future experiments involving further imaging and multi-site electrophysiological recordings. Nevertheless, we show here for the first time that some form of competition between various memory systems may exist at the time of occurrence of SPW-Rs, during the off-line states. If competitive or even mutually exclusive dynamic connectivity does actually exist it could provide low interference during the consolidation of multiple memory traces.

Another observation is the selective suppression of V1 activity during SPW-Rs, despite the overall positive BOLD responses in the other primary sensory and associational cortices. Such distinct deactivation of V1 may be the result of brief, selective suppression of the brain sites related to so-called ponto-geniculo-occipital (PGO) waves, that is, the phasic field potentials recorded from the pons, LGN, and V1 (ref. 47) during the hippocampal–cortical dialogue (see Supplementary Information).

The dynamics of regional fMRI responses suggest that an initial thalamic activity suppression is followed by signal increases in association cortices, then in hippocampus, and finally in parietal and early sensory cortices. Ripples were the only events that were significantly locked to the positive–negative transition phase of the local slow oscillation, at least in the delta-band cycles. This temporal structure may well reflect the systematic relationship between thalamocortical and hippocampal oscillations that is well known from several electrophysiological studies in animal and humans. As briefly mentioned above, neocortical slow wave oscillations were shown to temporally organize other cortical and hippocampal patterns[26,27,30–33], which themselves are temporally linked to spindles[24,34,35]. In addition, human SPW-Rs seem to be phase locked to hippocampal delta oscillations, indicating that the coupling between neocortical slow oscillations and SPW-Rs may be accomplished by the intermediate phase locking of ripples to the local, hippocampal delta-band activity, which is itself phase locked to neocortical slow oscillations[48,49]. Our current findings further support the idea that hippocampal delta provides an intermediate synchronization mechanism between cortex and hippocampus. However, it is surprising that such a synchronization occurs concurrently with the interruption of activity in a large number of other structures.

It is worth noting again here that both gamma and hpsigma events correlated with widespread (albeit of lesser spatial extent) modulations of brain areas, and that these modulations were primarily increases in the BOLD signal. As BOLD is known to be particularly sensitive to increase in gamma power[50], such widespread gamma-related activations may be indicative of episodic synchronous increases of subcortical and cortical regional gamma power that occur during the off-line states. Hippocampal transient high-gamma episodes have already been described in rats[38], but their functional significance is yet to be studied.

In summary, the present study demonstrates the advantage of using multimodal methodologies for the study of emerging properties of a complex system such as the brain. Ripples are characteristic hippocampal events, and their use as a 'trigger' has revealed up- and down-regulation of widespread network activity. Yet, a note of caution may be necessary to avoid misinterpretation of the functional importance of such events. Neither the activation maps nor the sequences of up- and down-regulation should be thought of indicating a causal relationship between the trigger event and the network activity changes. The state of widespread networks probably depends on a large number of variables (for example, activity changes in individual structures, or changes in inter-structure correlations), a subset of which may be eventually characterized following intensive future experimentation. The outcome of each experimental session may be conceived as a partially ordered sequence of system states, and such a sequence may indeed provide information related to memory. However, events in isolation are likely to be indicators rather than effectors of any cognitive capacity.

METHODS SUMMARY

All surgical and experimental procedures were approved by the local authorities (Regierungspraesidium, Tübingen Referat 35, Veterinärwesen) and were in full compliance with the guidelines of the European Community (EUVD 86/609/EEC) for the care and use of laboratory animals.

Received 3 June; accepted 24 September 2012.

1. Squire, L. R. Memory and the hippocampus: a synthesis from findings with rats, monkeys, and humans. *Psychol. Rev.* **99,** 195–231 (1992).
2. Eichenbaum, H. Declarative memory: insights from cognitive neurobiology. *Annu. Rev. Psychol.* **48,** 547–572 (1997).
3. Nadel, L. & Hardt, O. Update on memory systems and processes. *Neuropsychopharmacology* **36,** 251–273 (2011).
4. Buzsáki, G. Two-stage model of memory trace formation: a role for "noisy" brain states. *Neuroscience* **31,** 551–570 (1989).
5. Buzsáki, G. The hippocampo–neocortical dialogue. *Cereb. Cortex* **6,** 81–92 (1996).
6. Hasselmo, M. E. Neuromodulation and the hippocampus: memory function and dysfunction in a network simulation. *Prog. Brain Res.* **121,** 3–18 (1999).
7. Pennartz, C. M. A., Uylings, H. B. M., Barnes, C. A. & McNaughton, B. L. Memory reactivation and consolidation during sleep: from cellular mechanisms to human performance. *Prog. Brain. Res.* **138,** 143–166 (2002).
8. Eichenbaum, H. A cortical-hippocampal system for declarative memory. *Nature Rev. Neurosci.* **1,** 41–50 (2000).
9. Buzsáki, G., Horvath, Z., Urioste, R., Hetke, J. & Wise, K. High-frequency network oscillation in the hippocampus. *Science* **256,** 1025–1027 (1992).
10. O'Keefe, J. & Nadel, L. *The Hippocampus as a Cognitive Map* 114–152 (Oxford Univ. Press, 1978).
11. Skaggs, W. E. *et al.* EEG sharp waves and sparse ensemble unit activity in the macaque hippocampus. *J. Neurophysiol.* **98,** 898–910 (2007).
12. Axmacher, N., Elger, C. E. & Fell, J. Ripples in the medial temporal lobe are relevant for human memory consolidation. *Brain* **131,** 1806–1817 (2008).
13. Ylinen, A. *et al.* Sharp wave-associated high-frequency oscillation (200 Hz) in the intact hippocampus: network and intracellular mechanisms. *J. Neurosci.* **15,** 30–46 (1995).
14. Girardeau, G. & Zugaro, M. Hippocampal ripples and memory consolidation. *Curr. Opin. Neurobiol.* **21,** 452–459 (2011).
15. Wilson, M. A. & McNaughton, B. L. Reactivation of hippocampal ensemble memories during sleep. *Science* **265,** 676–679 (1994).
16. Kudrimoti, H. S., Barnes, C. A. & McNaughton, B. L. Reactivation of hippocampal cell assemblies: effects of behavioral state, experience, and EEG dynamics. *J. Neurosci.* **19,** 4090–4101 (1999).
17. Nádasdy, Z., Hirase, H., Czurko, A., Csicsvari, J. & Buzsaki, G. Replay and time compression of recurring spike sequences in the hippocampus. *J. Neurosci.* **19,** 9497–9507 (1999).
18. Skaggs, W. E. & McNaughton, B. L. Replay of neuronal firing sequences in rat hippocampus during sleep following spatial experience. *Science* **271,** 1870–1873 (1996).
19. Eschenko, O., Ramadan, W., Molle, M., Born, J. & Sara, S. J. Sustained increase in hippocampal sharp-wave ripple activity during slow-wave sleep after learning. *Learn. Mem.* **15,** 222–228 (2008).
20. O'Neill, J., Senior, T. J., Allen, K., Huxter, J. R. & Csicsvari, J. Reactivation of experience-dependent cell assembly patterns in the hippocampus. *Nature Neurosci.* **11,** 209–215 (2008).
21. Ramadan, W., Eschenko, O. & Sara, S. J. Hippocampal sharp wave/ripples during sleep for consolidation of associative memory. *PloS ONE* **4,** e6697 (2009).

22. Girardeau, G., Benchenane, K., Wiener, S. I., Buzsaki, G. & Zugaro, M. B. Selective suppression of hippocampal ripples impairs spatial memory. *Nature Neurosci.* **12,** 1222–1223 (2009).
23. Ego-Stengel, V. & Wilson, M. A. Disruption of ripple-associated hippocampal activity during rest impairs spatial learning in the rat. *Hippocampus* **20,** 1–10 (2010).
24. Siapas, A. G. & Wilson, M. A. Coordinated interactions between hippocampal ripples and cortical spindles during slow-wave sleep. *Neuron* **21,** 1123–1128 (1998).
25. Wierzynski, C. M., Lubenov, E. V., Gu, M. & Siapas, A. G. State-dependent spike-timing relationships between hippocampal and prefrontal circuits during sleep. *Neuron* **61,** 587–596 (2009).
26. Isomura, Y. *et al.* Integration and segregation of activity in entorhinal–hippocampal subregions by neocortical slow oscillations. *Neuron* **52,** 871–882 (2006).
27. Sirota, A., Csicsvari, J., Buhl, D. & Buzsaki, G. Communication between neocortex and hippocampus during sleep in rodents. *Proc. Natl Acad. Sci. USA* **100,** 2065–2069 (2003).
28. Steriade, M., Nunez, A. & Amzica, F. A novel slow (1 Hz) oscillation of neocortical neurons *in vivo*: depolarizing and hyperpolarizing components. *J. Neurosci.* **13,** 3252–3265 (1993).
29. McCormick, D. A. & Bal, T. Sleep and arousal—thalamocortical mechanisms. *Annu. Rev. Neurosci.* **20,** 185–215 (1997).
30. Mölle, M., Marshall, L., Gais, S. & Born, J. Grouping of spindle activity during slow oscillations in human non-rapid eye movement sleep. *J. Neurosci.* **22,** 10941–10947 (2002).
31. Amzica, F. & Steriade, M. The K-complex: its slow (1-Hz) rhythmicity and relation to delta waves. *Neurology* **49,** 952–959 (1997).
32. Battaglia, F. P., Sutherland, G. R. & McNaughton, B. L. Hippocampal sharp wave bursts coincide with neocortical "up-state" transitions. *Learn. Mem.* **11,** 697–704 (2004).
33. Mölle, M., Yeshenko, O., Marshall, L., Sara, S. J. & Born, J. Hippocampal sharp wave-ripples linked to slow oscillations in rat slow-wave sleep. *J. Neurophysiol.* **96,** 62–70 (2006).
34. Clemens, Z. *et al.* Temporal coupling of parahippocampal ripples, sleep spindles and slow oscillations in humans. *Brain* **130,** 2868–2878 (2007).
35. Axmacher, N., Mormann, F., Fernandez, G., Elger, C. E. & Fell, J. Memory formation by neuronal synchronization. *Brain Res. Rev.* **52,** 170–182 (2006).
36. Born, J. Slow-wave sleep and the consolidation of long-term memory. *World J. Biol. Psychiatry* **11,** 16–21 (2010).
37. Steriade, M. The corticothalamic system in sleep. *Front. Biosci.* **8,** d878–d899 (2003).
38. Sullivan, D. *et al.* Relationships between hippocampal sharp waves, ripples, and fast gamma oscillation: influence of dentate and entorhinal cortical activity. *J. Neurosci.* **31,** 8605–8616 (2011).
39. Paxinos, G., Huang, X. F., Petrides, M. & Toga, A. W. *The Rhesus Monkey Brain in Stereotactic Coordinates* (Elsevier, 2008).
40. Shmuel, A., Augath, M. A., Oeltermann, A. & Logothetis, N. K. Negative functional MRI response correlates with decreases in neuronal activity in monkey visual area V1. *Nature Neurosci.* **9,** 569–577 (2006).
41. Logothetis, N. K. *et al.* The effects of electrical microstimulation on cortical signal propagation. *Nature Neurosci.* **13,** 1283–1291 (2010).
42. Vincent, J. L. *et al.* Coherent spontaneous activity identifies a hippocampal–parietal mnemonic network. *J. Neurophysiol.* **96,** 3517–3531 (2006).
43. Poldrack, R. A. & Packard, M. G. Competition among multiple memory systems: converging evidence from animal and human brain studies. *Neuropsychologia* **41,** 245–251 (2003).
44. Schroeder, J. P., Wingard, J. C. & Packard, M. G. Post-training reversible inactivation of hippocampus reveals interference between memory systems. *Hippocampus* **12,** 280–284 (2002).
45. Oliveira, A. M., Hawk, J. D., Abel, T. & Havekes, R. Post-training reversible inactivation of the hippocampus enhances novel object recognition memory. *Learn. Mem.* **17,** 155–160 (2010).
46. Poldrack, R. A. & Rodriguez, P. How do memory systems interact? Evidence from human classification learning. *Neurobiol. Learn. Mem.* **82,** 324–332 (2004).
47. Mouret, J., Jeannero, M. & Jouvet, M. L'activité électrique du systeme visuel au cours de la phase paradoxale du sommeil chez le chat. *J. Physiol.* (*Paris*) **55,** 305–306 (1963).
48. Wolansky, T., Clement, E. A., Peters, S. R., Palczak, M. A. & Dickson, C. T. Hippocampal slow oscillation: a novel EEG state and its coordination with ongoing neocortical activity. *J. Neurosci.* **26,** 6213–6229 (2006).
49. Axmacher, N., Elger, C. E. & Fell, J. Memory formation by refinement of neural representations: the inhibition hypothesis. *Behav. Brain Res.* **189,** 1–8 (2008).
50. Logothetis, N. K. What we can do and what we cannot do with fMRI. *Nature* **453,** 869–878 (2008).

Supplementary Information is available in the online version of the paper.

Acknowledgements We thank D. Omer and M. Munk for reading the manuscript and for useful suggestions, D. Blaurock for English language corrections and editing, and P. Douay for help with the alert monkey experiments. This research was supported by the Max Planck Society. We apologize to those whose work we have not been able to cite for reasons of space.

Author Contributions N.K.L and O.E. designed the experiments and carried out research. N.K.L. analysed the data, wrote the manuscript and supervised the research. Y.M. carried out research and, together with M.B., contributed data analysis. M.A. and T.S. collected the physiology fMRI data, H.C.E. helped with all anatomical details required to define ROIs and enable three-dimensional registration of functional images to standard anatomical scans, and A.O. designed and developed all electronics and electrodes permitting concurrent multiple-contact electrophysiological recordings and fMRI.

Author Information Reprints and permissions information is available at www.nature.com/reprints. The authors declare no competing financial interests. Readers are welcome to comment on the online version of the paper. Correspondence and requests for materials should be addressed to N.K.L. (Nikos.Logothetis@tuebingen.mpg.de).